

Anomalous Hall Heat Current and Nernst Effect in the $\text{CuCr}_2\text{Se}_{4-x}\text{Br}_x$ Ferromagnet

Wei-Li Lee,¹ S. Watauchi,^{2,*} V. L. Miller,² R. J. Cava,² and N. P. Ong¹

¹*Department of Physics, Princeton University, New Jersey 08544, USA*

²*Department of Chemistry, Princeton University, New Jersey 08544, USA*

(Received 8 June 2004; published 22 November 2004)

In a ferromagnet, an anomalous Hall heat current, given by the off-diagonal Peltier term α_{xy} , accompanies the anomalous Hall current. By combining Nernst, thermopower, and Hall experiments, we have measured how α_{xy} varies with hole density and lifetime τ in $\text{CuCr}_2\text{Se}_{4-x}\text{Br}_x$. At low temperatures T , we find that α_{xy} is independent of τ , consistent with anomalous-velocity theories. Its magnitude is fixed by a microscopic geometric area $\mathcal{A} \sim 34 \text{ \AA}^2$. Our results are incompatible with some models of the Nernst effect in ferromagnets.

DOI: 10.1103/PhysRevLett.93.226601

PACS numbers: 72.15.Gd, 72.10.Bg, 72.15.Jf, 75.47.-m

In a ferromagnet, the anomalous Hall effect (AHE) is the appearance of a spontaneous Hall current flowing parallel to $\mathbf{E} \times \mathbf{M}$, where \mathbf{E} is the electric field and \mathbf{M} the magnetization [1]. Karplus and Luttinger (KL) [2] proposed that the AHE current originates from an anomalous-velocity term which is nonvanishing in a ferromagnet. The topological nature of the KL theory has been of considerable interest recently [3–6]. Experimentally, strong evidence for the dissipationless nature of the AHE current has been obtained in the spinel ferromagnet $\text{CuCr}_2\text{Se}_{4-x}\text{Br}_x$. Lee *et al.* [7] reported that, despite a 1000-fold increase in the resistivity ρ induced by varying the Br content x , the anomalous Hall conductivity (normalized per carrier and measured at 5 K) stays at the same value, in agreement with the KL prediction. A test of the anomalous-velocity theory against the AHE in Fe has also been reported [8].

It has long been known that an anomalous heat current density \mathbf{J}^Q also accompanies the AHE current in the absence of any temperature gradient [9,10]. In principle, \mathbf{J}^Q can provide further information on the origin of the AHE, but almost nothing is known about its properties. A weak heat current is a challenge to measure. Instead, one often performs the “reciprocal” Nernst experiment in which a temperature gradient $-\nabla T$ produces a transverse charge current, which is detected as a Nernst electric field \mathbf{E}_N parallel to $\mathbf{M} \times (-\nabla T)$. However, in previous Nernst experiments on ferromagnets [9–11], \mathbf{J}^Q was not found because other transport quantities were not measured. Combining the Nernst signal with the AHE resistivity ρ'_{xy} and the thermopower, we have determined how the transport quantity α_{xy} relevant to \mathbf{J}^Q varies in $\text{CuCr}_2\text{Se}_{4-x}\text{Br}_x$ as the hole density n_h and carrier lifetime τ are greatly changed under doping. We show that α_{xy} has a strikingly simple form, with its magnitude scaled by a microscopic geometric area \mathcal{A} .

We apply a gradient $-\nabla T \parallel \hat{\mathbf{x}}$ to an electrically isolated sample in a magnetic field $\mathbf{H} \parallel \hat{\mathbf{z}}$. Along $\hat{\mathbf{x}}$, the charge current driven by $-\nabla T$ is balanced by a backflow current

produced by a large E_x which is detected as the thermopower $S = E_x/|\nabla T|$. Along the transverse direction $\hat{\mathbf{y}}$, however, both E_x and $-\nabla T$ generate Hall-type currents. In general, the charge current in the presence of \mathbf{E} and $-\nabla T$ is $\mathbf{J} = \boldsymbol{\sigma} \cdot \mathbf{E} + \boldsymbol{\alpha} \cdot (-\nabla T)$, with $\boldsymbol{\sigma}$ and $\boldsymbol{\alpha}$ the electrical and thermoelectric (“Peltier”) conductivity tensors, respectively. Setting $J_y = 0$, we obtain the Nernst signal $e_N \equiv E_y/|\nabla T| = \rho \alpha_{xy} + \rho_{xy} \alpha$, where $\alpha \equiv \alpha_{xx}$ [12]. Hence, as noted, the Nernst signal results from the two distinct y -axis charge currents, $\alpha_{yx}(-\nabla T)$ and $\sigma_{yx}E_x$. In a ferromagnet, the former is our desired gradient-driven current, whereas the latter comprises the “dissipationless” AHE current and the weak ordinary Hall current.

In terms of the thermopower $S = \rho \alpha$ and Hall angle $\tan \theta_H = \rho_{yx}/\rho$, we may express α_{xy} as

$$\rho \alpha_{xy} = e_N + S \tan \theta_H. \quad (1)$$

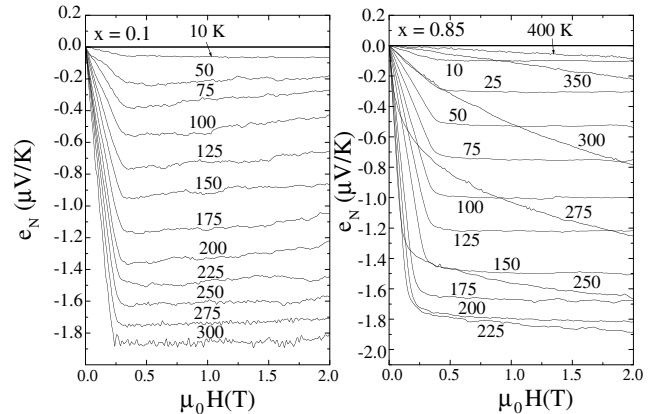


FIG. 1. Curves of the measured $e_N = E_y/|\nabla T|$ versus H in $\text{CuCr}_2\text{Se}_{4-x}\text{Br}_x$, with $x = 0.1$ (left panel) and 0.85 (right panel). In the ferromagnetic state below T_C , e_N saturates to a constant when H exceeds H_s , reflecting the M - H curve. The scaling factor Q_s increases rapidly as T increases from 10 K to T_C . In the right panel, e_N continues to scale as the M - H curve in the paramagnetic regime (275–400 K).

Hence, to find α_{xy} , we need to measure e_N , S , ρ_{xy} , and ρ . Knowing α_{xy} , we readily find the transverse heat current $J_y^Q = \tilde{\alpha}_{yx} E_x$, since $\tilde{\alpha}_{yx} = \alpha_{yx} T$ by Onsager reciprocity.

The spinel CuCr_2Se_4 is a conducting ferromagnet with a Curie temperature $T_C \sim 450$ K. Because the exchange between local moments in Cr is mediated by superexchange through 90° Cr-Se-Cr bonds rather than the carriers, T_C is not significantly reduced even when the hole population n_h drops by a factor of 30 under Br doping (M at 5 K actually increases by 20%) [7,13]. Using iodine vapor transport, we have grown crystals with x from 0.0 to 1.0. As x increases from 0 to 1, the value of ρ at 5 K increases by $\sim 10^3$, while ρ'_{xy}/n_h increases by $\sim 10^6$ [7]. The tunability of n_h and the robustness of M under doping make this system attractive for studying charge transport in a lattice with broken time-reversal symmetry. The behavior of ρ , M , and ρ'_{xy} versus x are described in Ref. [7].

Figure 1 shows profiles of e_N versus H at selected T in two samples with $x = 0.1$ and 0.85 and $T_C = 400$ and 275 K, respectively. As noted above, $e_N(T, H)$ is the sum of two terms, both of which scale as M . The magnitude $|e_N|$ initially increases as H rotates domains into alignment and then saturates to a constant for $H > H_s$, the saturation field. The sign of e_N —negative in all samples—reflects the sign of the dominant term [14].

In the sample with $x = 0.85$, the curves above T_C show that the scaling also holds in the paramagnetic regime where the susceptibility has the Curie-Weiss form $\chi \sim 1/(T - T_C)$ in weak H . In analogy with the Hall resistivity $\rho_{xy} = R_0\mu_0 H + R_s\mu_0 M$, with R_0 and R_s the ordinary and anomalous Hall coefficients, respectively, it is customary to express the scaling between the e_N - H and M - H curves by writing

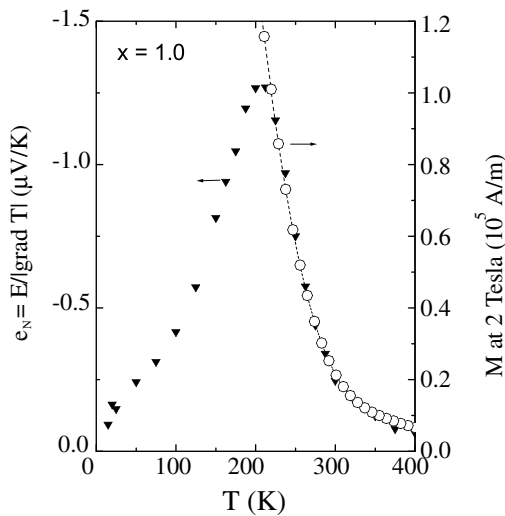


FIG. 2. The T dependence of the Nernst signal e_N (solid triangles) measured at 2 T in the sample with $x = 1.0$. Above T_C , e_N is compared with the paramagnetic magnetization M at 2 T (open circles).

$$e_N = Q_0\mu_0 H + Q_s\mu_0 M. \quad (2)$$

For $T < T_C$ in all samples, the Q_0 term cannot be resolved, so that $e_N \simeq Q_s\mu_0 M$. Moreover, below 50 K, M changes only weakly with x (by 20% over the whole doping range), so that the saturated value of the Nernst signal e_N^{sat} differs from Q_s by a factor that is only weakly x dependent.

The Nernst signal has very different characteristic behaviors below and above T_C . As an example, Fig. 2 shows e_N^{sat} measured at 2 T in the sample with $x = 1.0$ ($T_C = 210$ K). Between 5 and 100 K, e_N^{sat} increases linearly with T . Above 100 K, e_N^{sat} rises more steeply to a sharp peak 200 K, and then falls steeply above T_C . As noted, in the paramagnetic regime, the Nernst signal matches the behavior of M as a function of both T and H . Figure 2 shows that the T dependence of e_N closely follows that of $M = \chi H$ (both are measured at 2 T). The experiment shows that, in a gradient, fluctuations of the paramagnetic magnetization lead to a significant transverse electrical current that is proportional to the average magnetization (this has not been noted before, to our knowledge). We express the proportionality as

$$\alpha_{xy} = \beta M \quad (T > T_C), \quad (3)$$

where β is only weakly T dependent (it decreases by 5% between 250 and 400 K). The parameter β plays the important role of relating the magnitudes of the paramagnetic M and the transverse electronic current (through the Nernst signal). Its minuscule value ($\beta \simeq 2 \times 10^{-7} \text{ K}^{-1}$ at 250 K) reflects the strikingly weak coupling between the fluctuating M and e_N in a

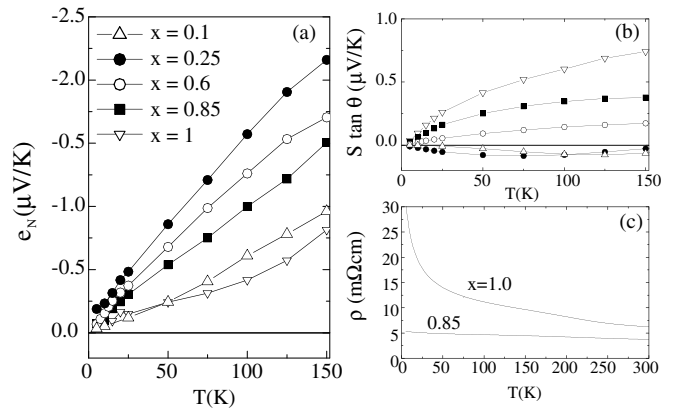


FIG. 3. (a) Curves of e_N versus T below 150 K in five samples with doping $0.1 \leq x \leq 1.0$ showing nominal T -linear behavior at low T ($H = 2$ T). The slopes vary nonmonotonically with x . (b) shows the Hall-current term $S \tan\theta_H$ measured in the same samples at $H = 2T$. For $x > 0.3$, $S \tan\theta_H$ is opposite in sign from e_N [the symbol key applies to both (a) and (b)]. (c) shows the sharp change in the ρ - T profiles in the samples with $x = 0.85$ and 1.0 ($H = 0$). At low T , ρ at 0.85 is metallic, but at 1.0 ρ reveals hopping between strongly localized states. See Ref. [7] for ρ versus T for $x < 0.85$.

ferromagnet; a sizeable $M \sim 10^5$ A/m produces a Nernst signal of only ~ 2 μ V/K. With the growth of long-range magnetic order below T_C , Eq. (3) ceases to be valid.

In the ferromagnetic state, we restrict our attention to the regime below 100 K, where e_N^{sat} is nominally linear in T . Figure 3(a) shows curves in this regime for the five samples studied. The slopes of the low- T curves are not monotonic in x . As x is increased from 0.1, the slope attains a maximum value at $x = 0.25$, and then decreases to a value close to its initial value when x reaches 1.0. This is perhaps not surprising since e_N involves transport quantities S , ρ , and ρ_{xy} with opposite trends versus x . By Eq. (1), we may find the curve of α_{xy} versus T by adding the curves e_N and $S \tan \theta_H$ [Fig. 3(b)] and dividing by ρ . The data in Figs. 3(a) and 3(b) show that these terms are opposite in sign for $x > 0.3$. With increasing x , their mutual cancellation suppresses α_{xy} strongly. In particular, at the largest x (0.85 and 1.0), the cancellation is nearly complete and α_{xy} is very small below 100 K; i.e., the observed e_N is nearly entirely from the AHE of the back-flow current. For $0.1 \leq x < 0.3$, $S \tan \theta_H$ is negligible and e_N largely reflects the behavior of α_{xy} . We exclude from our study the undoped compound CuCr_2Se_4 because e_N and ρ'_{xy} were not resolved at low T . These trends emphasize the importance of knowing all four transport quantities, instead of just e_N , to discuss \mathbf{J}^Q meaningfully.

Finally, the derived curves of α_{xy} versus T are shown in Fig. 4. In contrast to the nonmonotonic behavior of e_N versus x , α_{xy} varies linearly with T as $\alpha_{xy} = b(x)T + c$, where the slope $b(x)$ now decreases monotonically as x increases from 0.1 to 1.0 (Fig. 4). In all samples except $x = 0.25$, the parameter c —probably extrinsic in nature—is close to zero within our accuracy. The dependence of the parameter $b(x) = [\alpha_{xy}(T) - \alpha_{xy}(0)]/T$ on these two quantities is of main interest. Figure 4(b) compares how $b(x)$ and n_h (determined [7] from ρ_{xy} above T_C) vary with x . Whereas, at small x , the decrease in $b(x)$

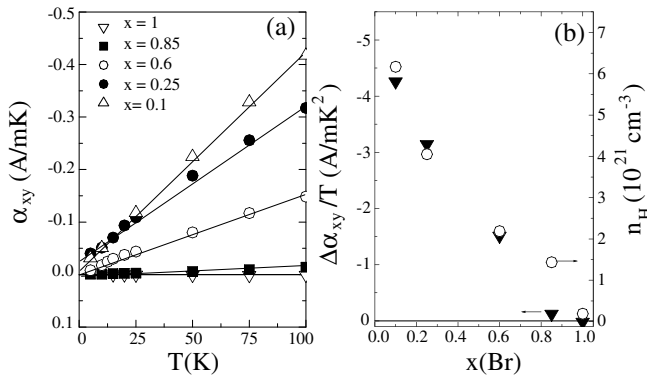


FIG. 4. (a) Curves of α_{xy} versus T obtained by adding e_N and $S \tan \theta_H$ [Eq. (1)]. The slope $b(x)$ now falls monotonically as x increases to 1.0. (b) compares how the slope $b(x) = \Delta \alpha_{xy}/T$ and n_h vary with x .

seems to match that of n_h , $b(x)$ falls much faster to zero at large x .

A striking relation between them becomes apparent if we plot one against the other. Figure 5 shows that, when x decreases below 0.85, $b(x)$ grows as a fractional power of $n_h - n_{h0}$ with n_{h0} a threshold density. This is consistent with $b(x)$ increasing as the density of states (DOS), viz., $b(x) \sim \mathcal{N}_F$. The DOS for the free-electron gas \mathcal{N}_F^0 (dashed curve) has a slightly stronger curvature than the data. Interestingly, the occurrence of the threshold doping at $x = 0.85$ accounts well for a puzzling change in the resistivity behavior when x exceeds 0.85 [Fig. 3(c)]. In general, slowly increasing x causes the resistivity profiles to change systematically, reflecting slight decreases in both n_h and ℓ_0 (mean-free path). However, between 0.85 and 1.0, the change is sudden and striking. At $x = 0.85$, ρ is T independent below 100 K consistent with a disordered metal. By contrast, at 1.0, ρ rises monotonically with decreasing T [Fig. 3(c)]. Between 300 and 4.2 K, ρ increases from 6.3 to 32 m Ω cm. At low T , conductivity proceeds by hopping between strongly localized states in an impurity band. Figure 5 confirms that we reach the extremum of the hole band near $x = 0.85$. Further removal of carriers ($x \rightarrow 1$) affects states within the impurity band.

Knowing n_h and ρ at each x , we may determine the mean-free path ℓ_0 in the impurity-scattering regime. Between $x = 0.1$ and 1.0, ℓ_0 decreases by a factor of 40. This steep decrease has no discernible influence on $b(x)$. Combining these factors then, we have $\alpha_{xy} = gT \mathcal{N}_F$, where g is independent of ℓ_0 . We may boil down α_{xy} to the measurement of an “area” \mathcal{A} by writing

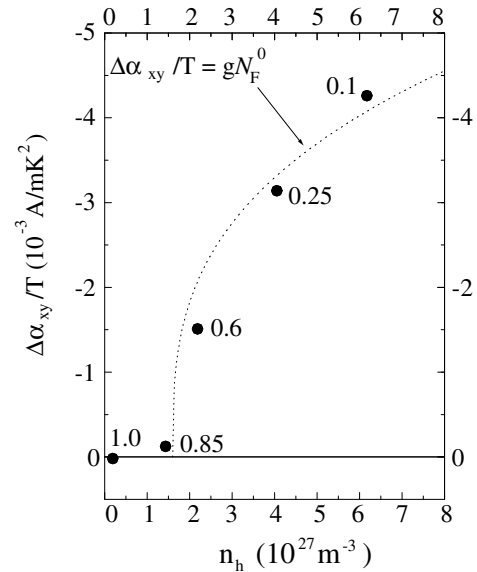


FIG. 5. Plot of $b(x) = \Delta \alpha_{xy}/T$ against n_h showing that for samples with $x \leq 0.85$ $b(x)$ increases as a fractional power of $n_h - n_{h0}$. The dashed line is $\Delta \alpha_{xy}/T = g \mathcal{N}_F^0$, with $g = 9.77 \times 10^{-50}$ in SI units.

$$\alpha_{xy} = \mathcal{A} \frac{ek_B^2 T}{\hbar} \mathcal{N}_F \quad (T \ll T_C), \quad (4)$$

with k_B Boltzmann's constant and e the electron charge. The value of g gives $\mathcal{A} = 33.8 \text{ \AA}^2$ if we assume $\mathcal{N}_F \sim \mathcal{N}_F^0$. As the anomalous Hall heat current produced by $\mathbf{E} \parallel \hat{\mathbf{x}}$ is $J_y^Q = \alpha_{yx} TE$, it shares the simple form in Eq. (4). The ratio $J_y^Q/J_y \sim T^2$, as expected for a Fermi gas.

We briefly sketch the anomalous-velocity theory [2–4]. In a periodic lattice, the position operator for an electron is the sum $\mathbf{x} = \mathbf{R} + \mathbf{X}(\mathbf{k})$, where \mathbf{R} locates a unit cell, while $\mathbf{X}(\mathbf{k})$ locates the intracell position [15]. A finite $\mathbf{X}(\mathbf{k})$ implies that \mathbf{x} does not commute with itself. Instead, we have [15] $[x_j, x_k] = i\epsilon^{jkm}\Omega_m$, with ϵ^{jkm} the antisymmetric tensor, which implies the uncertainty relation $\Delta x_j \Delta x_k \sim \Omega$. The ‘‘Berry curvature’’ $\mathbf{\Omega}(\mathbf{k}) = \nabla_{\mathbf{k}} \times \mathbf{X}$ is analogous to a magnetic field in \mathbf{k} space [16]. In the presence of \mathbf{E} , $\mathbf{\Omega}$ adds a term that is the analog of the Lorentz force to the velocity $\mathbf{v}_{\mathbf{k}}$, viz.,

$$\hbar \mathbf{v}_{\mathbf{k}} = \nabla \epsilon(\mathbf{k}) - \mathbf{E} \times \mathbf{\Omega}(\mathbf{k}). \quad (5)$$

The anomalous-velocity term in Eq. (5) immediately implies the existence of a spontaneous Hall current $\mathbf{J}_H = -2e \sum_{\mathbf{k}} f_{\mathbf{k}}^0 \mathbf{E} \times \mathbf{\Omega}(\mathbf{k})$, where $f_{\mathbf{k}}^0$ is the unperturbed distribution [2–4,8,15]. The unconventional form of the current—notably the absence of any lifetime dependence—has made the KL theory controversial for decades [1,17]. However, strong support has been obtained from the measurements of Lee *et al.* [7] showing that the normalized AHE conductivity σ'_{xy}/n_h in $\text{CuCr}_2\text{Se}_{4-x}\text{Br}_x$ is unchanged despite a 1000-fold increase in ρ .

In general, the off-diagonal term α_{xy} is related to the derivative of σ_{xy} at the chemical potential μ , viz., $\alpha_{xy} = (\pi^2/3)(k_B^2 T/e)[\partial \sigma_{xy}/\partial \epsilon]_{\mu}$ [12]. Using the result [7] that σ'_{xy} is linear in n_h but independent of ℓ_0 , and $[\partial n_h/\partial \epsilon]_{\mu} = \mathcal{N}_F$, we see that $\alpha_{xy} \sim T \mathcal{N}_F$, consistent with Eq. (4). (By contrast, we note that the skew-scattering model [17] would predict $\sigma'_{xy} \sim n_h \ell_0$ and $\alpha_{xy} \sim T \mathcal{N}_F \ell_0$.)

Finally, \mathcal{A} in Eq. (4) has the value 34 \AA^2 . If Eq. (5) is indeed the origin of α_{xy} , \mathcal{A} must be roughly the scale of $\Omega \sim \Delta x_j \Delta x_k$. Hence the value $\mathcal{A} \sim \frac{1}{3} \times$ the unit-cell area seems reasonable (the lattice spacing here is 10.33 \AA). While a quantitative comparison requires knowledge of $\mathbf{\Omega}(\mathbf{k})$ over the Brillouin zone, the simple form of Eq. (4) seems to provide valuable insight on the anomalous heat current.

A previous calculation of the Nernst coefficient was based on the ‘‘side-jump’’ model [18]. On scattering from an impurity, the carrier suffers a small sideways displacement δ to give on average $\tan \theta_H = \delta/\ell_0$. This was used to derive $Q_s \sim T(k_F \ell)^{-1}$. In our experiment, $k_F \ell$ falls monotonically, with increasing x , while e_N rises to a broad maximum near 0.25 before falling. Hence our experiment is in essential conflict with the side-jump

model. From earlier experiments [11], an empirical form $Q_s = -(a + b'\rho)T$ has been inferred (a, b' are constants). This is not borne out in our data.

Combining Nernst, Hall, and thermopower experiments on the ferromagnet $\text{CuCr}_2\text{Se}_{4-x}\text{Br}_x$, we have determined how α_{xy} (hence \mathbf{J}^Q) changes as a function of n_h and τ . At low T , we find that α_{xy} follows the strikingly simple form $\alpha_{xy} \sim \mathcal{A} T \mathcal{N}_F$, consistent with the anomalous-velocity theory for the AHE (Fig. 4). In addition, a direct relation [Eq. (3)] between M and α_{xy} is observed in the paramagnetic regime above T_C .

We acknowledge support from the U.S. National Science Foundation (Grant No. DMR 0213706).

*Permanent address: Center for Crystal Science and Technology, University of Yamanashi, 7 Miyamae, Kofu, Yamanashi 400-8511, Japan.

- [1] For a review, see *The Hall Effect in Metals and Alloys*, edited by Colin Hurd (Plenum, New York, 1972), p. 153.
- [2] R. Karplus and J.M. Luttinger, Phys. Rev. **95**, 1154 (1954); J.M. Luttinger, Phys. Rev. **112**, 739 (1958).
- [3] Ganesh Sundaram and Qian Niu, Phys. Rev. B **59**, 14 915 (1999).
- [4] M. Onoda and N. Nagaosa, J. Phys. Soc. Jpn. **71**, 19 (2002).
- [5] S. Murakami, N. Nagaosa, and S.C. Zhang, Science **301**, 1348 (2003).
- [6] T. Jungwirth, Qian Niu, and A.H. MacDonald, Phys. Rev. Lett. **88**, 207208 (2002).
- [7] Wei-Li Lee, Satoshi Watauchi, R. J. Cava, and N. P. Ong, Science **303**, 1647 (2004).
- [8] Yugui Yao *et al.*, Phys. Rev. Lett. **92**, 037204 (2004).
- [9] Alpheus W. Smith, Phys. Rev. **17**, 23 (1921); R. P. Ivanova, Fiz. Met. Metalloved. **8**, 851 (1959).
- [10] For a table of Nernst data, see *Handbook of Physical Quantities*, edited by Igor S. Grigoriev and Evgenii Z. Meilikhov (CRC Press, Boca Raton, FL, 1997), p. 904.
- [11] E. I. Kondorskii, Sov. Phys. JETP **18**, 351 (1964); E. I. Kondorskii and R. P. Vasileva, Sov. Phys. JETP **18**, 277 (1964).
- [12] Yayu Wang *et al.*, Phys. Rev. B **64**, 224519 (2001).
- [13] K. Miyatani *et al.*, J. Phys. Chem. Solids **32**, 1429 (1971).
- [14] In our convention, the sign of e_N is that of the Nernst signal of vortex flow in a superconductor [12]; viz., e_N is positive if $\mathbf{E}_N \parallel \mathbf{H} \times (-\nabla T)$.
- [15] E. N. Adams and E. I. Blount, J. Phys. Chem. Solids **10**, 286 (1959).
- [16] In terms of Bloch functions $\psi_{n\mathbf{k}} = e^{i\mathbf{k}\cdot\mathbf{r}} u_{n\mathbf{k}}$, the matrix element of the intracell operator $\mathbf{X}(\mathbf{k}) = i \int d^3 r u_{n\mathbf{k}}^* \nabla_{\mathbf{k}} u_{n\mathbf{k}}$ has the form of a Berry gauge potential whose line integral gives a phase accumulation $\gamma = \oint d\mathbf{k} \cdot \mathbf{X}(\mathbf{k})$ that reflects motion in an effective magnetic field $\mathbf{\Omega} = \nabla_{\mathbf{k}} \times \mathbf{X}(\mathbf{k})$ existing in \mathbf{k} space.
- [17] J. Smit, Physica (Amsterdam) **21**, 877 (1955); Phys. Rev. B **8**, 2349 (1973).
- [18] L. Berger, Phys. Rev. B **2**, 4559 (1970); **5**, 1862 (1972).